BJ www.biochemj.org

BJ Structure

Biochem. J. (2011) **434**, 391–398 (Printed in Great Britain) doi:10.1042/BJ20101667

Spectroscopic and magnetic studies of wild-type and mutant forms of the Fe(II)- and 2-oxoglutarate-dependent decarboxylase ALKBH4

Linn G. BJØRNSTAD, Giorgio ZOPPELLARO, Ane B. TOMTER, Pål Ø. FALNES[1] and K. Kristoffer ANDERSSON[1]

Department of Molecular Biosciences, University of Oslo, P.O. Box 1041, Blindern, NO-0316 Oslo, Norway

The Fe(II)/2OG (2-oxoglutarate)-dependent dioxygenase superfamily comprises proteins that couple substrate oxidation to decarboxylation of 2OG to succinate. A member of this class of mononuclear non-haem Fe proteins is the *Escherichia coli* DNA/RNA repair enzyme AlkB. In the present work, we describe the magnetic and optical properties of the yet uncharacterized human ALKBH4 (AlkB homologue). Through EPR and UV–visible spectroscopy studies, we address the Fe-binding environment of the proposed catalytic centre of wild-type ALKBH4 and an Fe(II)-binding mutant. We could observe a novel unusual Fe(III) high-spin EPR-active species in the presence of sulfide with a g_{max} of 8.2. The Fe(II) site was probed with NO. An intact histidine-carboxylate site is necessary for productive Fe binding. We also report the presence of a unique cysteine-rich motif conserved in the N-terminus of ALKBH4 orthologues, and investigate its possible Fe-binding ability. Furthermore, we show that recombinant ALKBH4 mediates decarboxylation of 2OG in absence of primary substrate. This activity is dependent on Fe as well as on residues predicted to be involved in Fe(II) co-ordination. The present results demonstrate that ALKBH4 represents an active Fe(II)/2OG-dependent decarboxylase and suggest that the cysteine cluster is involved in processes other than Fe co-ordination.

Key words: AlkB, AlkB homologue (ALKBH4), EPR, non-haem Fe, UV–visible spectroscopy.

INTRODUCTION

The superfamily of Fe(II) and 2OG (2-oxoglutarate, also known as α-ketoglutarate)-dependent dioxygenases (Pfam accession number PF03171) is the largest known non-haem Fe protein family able to carry out hydroxylation reactions of unactivated C–H groups. These enzymes act on a variety of substrates [1,2], and the reaction occurs by reductive activation of molecular oxygen coupled with decarboxylation of the co-substrate 2OG to succinate [3–5]. Within the oxidation process through an Fe(IV)O intermediate, one of the oxygen atoms from O_2 is incorporated into the succinate moiety and the other becomes a hydroxy group in the product [3–5]. The catalytically active site is formed by a mononuclear non-haem Fe centre co-ordinated, in general, by two histidine residues and one carboxylate moiety [6–9]. This site is responsible for the binding of 2OG as well as dioxygen. During turnover, the Fe(II) hexa-co-ordinated states change to a final penta-co-ordinated state, with an open oxygen co-ordination site [6–9], as observed in the three-dimensional structure of the deacetoxycephalosporin C synthase with Fe(II) and 2OG bound (PDB code 1RXG), the first structurally characterized member of this family [10]. However, when uncoupled turnover of 2OG takes place, either in the absence of natural substrates or due to incorrect orientation of substrates in the active site, decomposition of 2OG into succinate and CO_2 may lead to enzyme deactivation.

The Fe(II)/2OG dioxygenase AlkB from *Escherichia coli* is a repair enzyme, which is induced as part of the adaptive response to alkylation damage. AlkB catalyses demethylation of 1meA (1-methyladenine) and 3meC (3-methylcytosine) in DNA in a reaction where the methyl group is hydroxylated and then released as formaldehyde, thereby regenerating the normal base [11,12]. Additionally, AlkB repairs the structurally analogous lesions 1meG (1-methylguanine) and 3meT (3-methylthymidine) and the bulkier exocyclic etheno and ethano adducts [13–17]. Moreover, AlkB also displays activity on methylated RNA [18]. A bioinformatics analysis revealed eight different mammalian ALKBHs (AlkB homologues), denoted ALKBH1–8 [19], and a more recent study has demonstrated FTO (fat mass and obesity-associated protein) [20] to be a functional ALKBH and thus the ninth member of this family [21]. AlkB-like *in vitro* repair activities have been reported for ALKBH1 [22], ALKBH2, ALKBH3 [23] and FTO [21], but only ALKBH2 has been convincingly demonstrated to function as a repair enzyme *in vivo* [24,25].

Recently, it has become clear that the ALKBH proteins are involved in processes other than DNA/RNA repair, as ALKBH8 has been demonstrated to be a tRNA modification enzyme [26–28] and ALKBH1 has been implicated in gene regulation [29]. ALKBH4–ALKBH7 remain completely uncharacterized; in fact, nothing is known about their ability to bind Fe-metal ion, the nature of the so-formed active site(s) and their optical/magnetic fingerprints. From the sequence alignment of putative ALKBH4 orthologues from various organisms, we noted the presence of a cluster of four highly conserved cysteine residues very close to the N-terminus (Figure 1). This cluster is not present in AlkB, and we reasoned that it potentially constitutes a complementary Fe–S binding site. In order to clearly elucidate the nature of the Fe-metal binding by human ALKBH4 in its anticipated binding triad of two histidine residues and one carboxylate motif (His^{169}-Asp^{171}-His^{254}) (Figure 2) and to address the possible role of the cysteine cluster as an additional Fe–S centre, in the present work we studied the enzymatic activities and the optical and magnetic fingerprints

Abbreviations used: ALKBH, AlkB homologue; FTO, fat mass and obesity-associated protein; GST, glutathione transferase; ICP-AEP, inductively coupled plasma atomic emission spectroscopy; IPNS, isopenicillin N synthase; IPTG, isopropyl β-D-thiogalactopyranoside; $MV^{\bullet+}$, Methyl Viologen radical cation; 2OG, 2-oxoglutarate; PAH, phenylalanine hydroxylase; 4,5-PCD, protocatechuate 4,5-dioxygenase; TauD, taurine dioxygenase; UV–Vis, UV–visible; ZFS, zero-field splitting.

[1] Correspondence may be addressed to either of these authors (email k.k.andersson@imbv.uio.no or pal.falnes@imbv.uio.no).

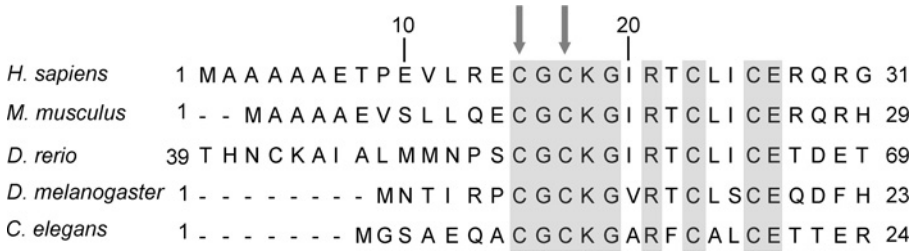

Figure 1 Sequence alignment of the N-terminal part of putative ALKBH4 orthologues from different organisms

Arrows indicate the cysteine residues subjected to mutagenesis (C15A/C17A). GenBank® Identifier (gi) numbers of the displayed sequences are as follows: 8923019 (*Homo sapiens*), 81905645 (*Mus musculus*), 68372246 (*Danio rerio*), 24583140 (*Drosophila melanogaster*) and 25148697 (*Caenorhabditis elegans*). The alignment was generated using the MAFFT algorithm [48] and displayed in Jalview [49].

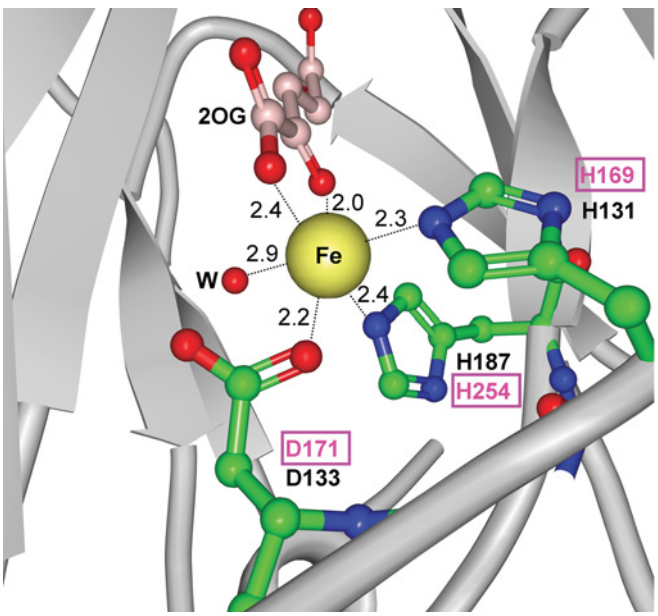

Figure 2 Close-up view of the catalytic centre of AlkB in the presence of bound 2OG (PDB code 2FD8) [50]

The amino acid residues that complex the Fe metal are indicated in black (H131, D133, H187). A water molecule (W) weakly interacting with the Fe ion (Fe–H_2O = 2.9 Å; 1 Å = 0.1 nm) is also shown. The amino acid residues of ALKBH4 thought to form a similar Fe metal-binding triad (H169, D171, H254) [19] are indicated by boxed magenta labels.

[UV–Vis (UV–visible)/EPR] of the wild-type protein and of two mutant derivatives. One mutant (C15A/C17A) contained an abrogated cysteine cluster, whereas the motif putatively involved in Fe(II) binding was destroyed in the other (H169A/D171A).

MATERIALS AND METHODS

Plasmid construction and site-specific mutagenesis of ALKBH4

The cDNA encoding human ALKBH4 was amplified by PCR and inserted between the NdeI and BamHI sites of the expression vector pET-28a (Novagen). The QuikChange™ Site-Directed Mutagenesis Kit (Stratagene) was used for generation of ALKBH4 mutants. To generate the pET-H169A/D171A plasmid, the primers 5′-CTGCCATTGACCCCGCCCTGGCCGACGCCTGGCTG-3′ and 5′-CAGCCAGGCGTCGGCCAGGGCGGGGTCAATGGCAG-3′ were used, and the primers 5′-CGAAGTCCTTCGGGAAGCCGGTGCCAAGGGCATCCGGACC-3′ and 5′-GGTCCGGATGCCCTTGGCACCGGCTTCCCGAAGGACTTCG-3′ were used for generation of the plasmid pET-C15A/C17A (underlining indicates mutation sites). Plasmids encoding GST (glutathione transferase)-tagged mutants were obtained by subcloning the mutated cDNA fragments into the vector pGEX-6P-2 (GE Healthcare), resulting in the plasmids pGEX-H169A/D171A and pGEX-C15A/C17A respectively (BamHI and EcoRI sites were used for H169A/D171A, and BamHI and SalI sites were used for C15A/C17A). All PCR-generated fragments were verified by DNA sequencing.

Purification of ALKBH4 and mutant proteins

Plasmids were transformed into the *E. coli* strain BL21-CodonPlus(DE3)-RIPL (Stratagene), and protein expression was induced by the addition of 0.075–0.1 mM IPTG (isopropyl β-D-thiogalactopyranoside). Cells were disrupted by French press treatment [two passages through a standard FRENCH® pressure cell (Thermo Electron) at a working pressure of 1000 psi (1 psi = 6.9 kPa)], and proteins were purified from clarified lysates using affinity purification. For spectroscopic analysis, ALKBH4 and mutants were expressed as GST-fusion proteins and purified using glutathione–Sepharose 4B medium (GE Healthcare). The GST tag was removed by on-column enzymatic cleavage using PreScission protease (GE Healthcare), and HiTrap Desalting columns (GE Healthcare) were used for buffer exchange (50 mM Hepes, pH 7.0, and 100 mM KCl). His_6-tagged AlkB proteins for decarboxylation assays were purified using TALON® Metal Affinity Resin (Clontech). Proteins were analysed by SDS/4–12 % PAGE and subsequent Coomassie Brilliant Blue staining. The metal content (Fe) in the protein preparations was probed by ICP-AEP (inductively coupled plasma atomic emission spectroscopy), with detection at 238.204 nm for the Fe ion emission line.

Assay for decarboxylation of 2OG to succinate

The reactions were performed as described previously [14]. Briefly, reaction mixtures of 50 μl contained 50 mM Hepes, pH 7.5, 4 mM ascorbic acid, 160 μM 2OG (10 % [5–^{14}C]2OG), 80 μM $FeSO_4$ (when indicated) and His_6-tagged ALKBH4 (500 pmol of wild-type or mutants) or *E. coli* His–AlkB (100 pmol). EDTA (1 mM) was added to samples without $FeSO_4$. Reactions were incubated at 37 °C for 30 min. The amount of [1–^{14}C]succinate formed was measured by scintillation counting after precipitation of the remaining 2OG with 2,4-DNPH (2,4-dinitrophenylhydrazine).

Metal-reconstitution procedures and spectroscopic measurements

Concentrated (<300 μM) protein solutions were obtained by centrifugal filter devices (Microcon YM-10) in 50 mM Hepes, pH 7.0, and were then made anaerobic in airtight vessels by several rounds of vacuum treatment and argon exchange using the Schlenk technique [29a]. The minimum amount ($\leqslant$2 mol per mol of protein) of a freshly prepared anaerobic solution of $Na_2S_2O_4$ (5.7 mM in 50 mM Hepes, pH 7.0) was then added to the protein solutions using airtight syringes. Stoichiometric amounts of Fe(II) ammonium sulfate were added to the protein samples in a similar way, using anaerobic stocks. In some cases, small amounts ($\sim$20 μM) of Methyl Viologen were added in order to monitor that strict anaerobic conditions were maintained within reconstitution procedures. Anaerobic solutions of 2OG and Na_2S in 50 mM Hepes, pH 7.0, were freshly prepared and added to the protein samples at a 10-fold excess. These solutions were transferred to quartz EPR tubes through airtight syringes that were maintained under argon, and then the tubes were sealed with Precision Seal® rubber septa (Sigma–Aldrich). Nitric oxide (NO) gas was added through airtight syringes directly into the quartz EPR tubes containing the sample protein, or to airtight 1 cm optical path quartz cuvettes. Samples were maintained at cold temperatures ($\leqslant$10 °C). Sample oxidation was obtained by air exposure followed by slow injection of O_2 ($\sim$90 % purity, $\sim$5 min). In the experiments employing reconstitution in the presence of 2OG/Na_2S/$Na_2S_2O_4$, sample oxidation was obtained by injection of 50 μl of O_2-saturated 50 mM Hepes, pH 7.0, into EPR tubes containing 100 μl of protein sample, followed by fast quenching in liquid nitrogen. The low-temperature EPR spectra were acquired on a Bruker Elexsys 560 instrument equipped with a dual-band X-resonator (Bruker) and by using a ESR900 He-flow cryostat (Oxford Instruments). UV–Vis spectra were recorded on a HP 8452A diode-array spectrophotometer (Hewlett Packard).

RESULTS AND DISCUSSION

Decarboxylation activity of ALKBH4 and mutant proteins towards 2OG

Like several of the Fe(II)/2OG dioxygenases, *E. coli* AlkB possesses the ability to perform decarboxylation of 2OG to succinate even in the absence of primary substrate [11,12]. Since the primary substrate of ALKBH4 is still unknown, we took advantage of such uncoupled co-substrate conversion to test the *in vitro* enzymatic activity of ALKBH4. For this purpose, recombinant His_6-tagged ALKBH4 and two mutants were purified from *E. coli* (Figure 3A) and subsequently assayed for 2OG decarboxylation activity. Indeed, ALKBH4 was able to catalyse succinate formation in the presence of the co-factor Fe(II), although not to the same extent as AlkB (Figure 3B). The decarboxylation activity was reduced to background levels when Fe(II) was not included, demonstrating the requirement for Fe, which is indicative of AlkB proteins. Likewise, the H169A/D171A mutant was devoid of the ability to perform 2OG turnover. The C15A/C17A mutant displayed a decarboxylation activity similar to that of the wild-type ALKBH4 protein, suggesting that the cysteine motif is not involved in Fe(II) co-ordination. Taken together, these results experimentally confirmed that ALKBH4 is a Fe(II)/2OG-dependent decarboxylase.

Spectroscopic fingerprints of the Fe catalytic centre of ALKBH4 and mutant proteins probed by EPR

The electronic/magnetic fingerprints of the native and mutant proteins were then addressed by low-temperature EPR

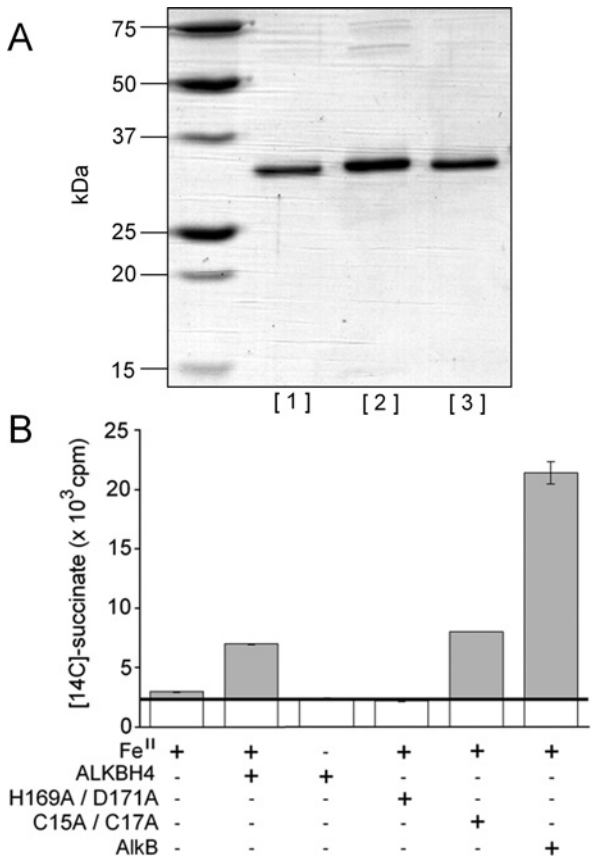

Figure 3 2OG decarboxylation activity of ALKBH4

(**A**) SDS/PAGE (4–12 %) analysis of purified recombinant proteins. Lane 1, ALKBH4; lane 2, H169A/D171A mutant; and lane 3, C15A/C17A mutant. The molecular mass in kDa is indicated on the left-hand side. (**B**) ALKBH4 (500 pmol of wild-type or mutant protein) or AlkB (100 pmol) was incubated in the presence of [5–^{14}C]2OG and the resulting [^{14}C]succinate formed was measured by scintillation counting. Fe(II) was added as indicated. Results are means $\pm$ S.D. of duplicate samples. The bold line shows the averaged background value (2500 c.p.m.).

measurements down to cryogenic temperatures. We probed different conditions where the metal co-ordination environment of Fe reconstituted ALKBH4, and mutant proteins were analysed both in the reduced [Fe(II)] and oxidized [Fe(III)] states, as well as in the presence or absence of 2OG/succinate. The results are summarized in Table 1. It should be noted that the isolated proteins (ALKBH4 and mutants), even when kept in iced-cooled solutions (4 °C), aggregated and then precipitated at concentrations higher than 0.5 mM. The process was accelerated greatly when an excess (e.g. 5-fold) of dithionite was added to the solution when anaerobic Fe(II)-reconstitution procedures were carried out. Nevertheless, low protein concentrations (<0.3 mM) and a slight excess of $Na_2S_2O_4$ (approx. twice greater) allowed efficient reconstitution of the apo-proteins with the Fe(II) metal ion, hence avoiding precipitation. The purified ALKBH4 protein, in the absence of added cofactors, gave rise to an extremely weak high-spin Fe(III) signal at $g \approx 4.3$ (Figure 4A). This resonance did not increase upon addition of oxidants (e.g. Na_2IrCl_6). This agrees with the ICP-AES findings that indicated the presence of Fe traces only in the purified protein. Traces of Cu(II) ion as an impurity (around $g \approx 2.1$) were also detected, with relative amounts that changed from sample to sample. When ALKBH4 and the C15A/C17A and H169A/D171A mutants were incubated with stoichiometric amounts of Fe(II) under reducing conditions, either in the presence or absence of 2OG/succinate, the recorded

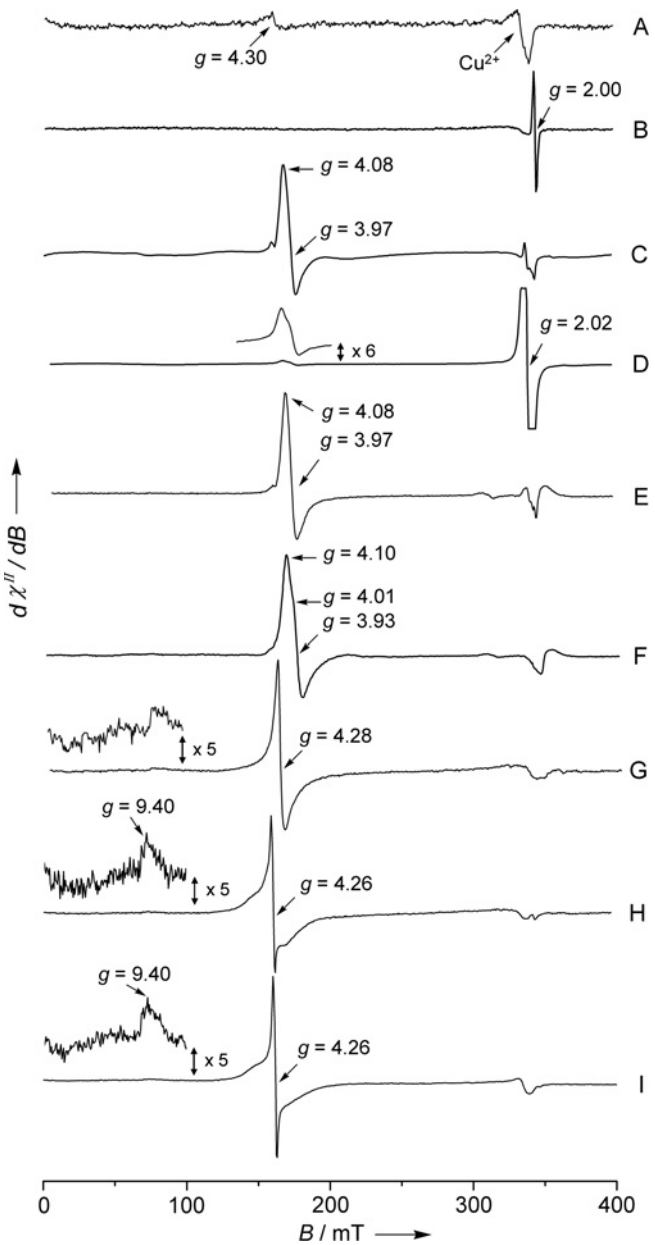

Figure 4 EPR spectroscopy of Fe-reconstituted ALKBH4 and mutant proteins

X-band EPR spectra of (**A**) purified ALKBH4, (**B**) ALKBH4 after incubation with stoichiometric amounts of Fe(II), (**C**) ALKBH4/Fe(II) after addition of NO, (**D**) the H169A/D171A/Fe(II) mutant after addition of NO, (**E**) ALKBH4/Fe(II) after addition of NO in the presence of 2OG, (**F**) ALKBH4/Fe(II) after addition of NO in the presence of succinate, (**G**) the H169A/D171A/Fe(II) mutant after addition of O_2, (**H**) ALKBH4/Fe(II)/2OG after addition of O_2 and (**I**) ALKBH4/Fe(II) after addition of O_2. Protein concentrations were 180–200 μM in 50 mM Hepes, pH 7.0. The measurements were performed at $T = 8.0 \pm 0.5$ K (approx. –265 °C) with the following parameters: frequency, 9.67 GHz; modulation frequency, 100 KHz; modulation amplitude, 0.7 mT; gain, 55 dB; time constant, 81.92 ms; sweep time, 323 s; microwave power, 0.4–0.8 mW. Two scans were accumulated and averaged; cavity quality factor $Q = 4300$–4600. Note that in (**B**) the sharp signal at $g = 2.00$ arises from $MV^{\bullet+}$, which was used as an internal indicator to probe the attainment of rigorous anaerobic conditions.

low-temperature EPR spectra did not show any Fe-related signal (Figure 4B). It is important to note that the only resonance signal emerging in the spectra was always associated with the presence of $MV^{\bullet+}$ (Methyl Viologen radical cation) ($g = 2.00$ in Figure 4B), which was used as an internal indicator to probe the attainment of rigorous anaerobic conditions. These results can be interpreted at X-band EPR with either (i) an integer-spin system having a high-spin Fe(II) state ($S = 2$, where S is the ground-state spin) characterized by a large axial ZFS (zero-field splitting) term called δ in EPR or Δ in MCD (magnetic CD), as it occurs in many mononuclear non-haem Fe proteins where such configuration is usually not spectroscopically accessible, or alternatively (ii) by a low-spin Fe(II) state ($S = 0$) [1,2,30]. NO has been successfully used as a probe for such centres [31], since it can convert the $S = 2$ species into an EPR-active $S = 3/2$ species, as observed, for example, in IPNS (isopenicillin N synthase) [32], in extradiol-cleaving catechol dioxygenases such as 2,3-CTD (catechol 2,3-dioxygenase) and 4,5-PCD (protocatechuate 4,5-dioxygenase) [33,34], as well as in non-haem Fe model complexes [35]. Upon anaerobic addition of NO to Fe(II)-reconstituted ALKBH4 and C15A/C17A protein in the absence of 2OG, a strong axial EPR signal centred at a g_{eff} of 3.97 developed (g-tensor components at $g_1 = 4.08$, $g_2 = 3.97$ and $g_3 = 2.00$), together with a second asymmetric resonance at $g \approx 2.00$ (Figure 4C). The latter signal contained features characteristic of a small amount of NO radical being trapped in the frozen matrix solution. Similarly, when anaerobic reconstitution of the ALKBH4 and C15A/C17A proteins was carried out with both Fe(II) and a 10-fold excess of 2OG, a strong axial resonance signal centred at $g_{eff} = 3.97$ developed after NO addition, being accompanied by a small highly asymmetric signal around $g \approx 2.00$ (Figure 4E). Analogous spurious signals at $g \approx 2.00$ are found in other non-haem Fe proteins, such as 4,5-PCD [36] and IPNS [32]. Therefore in both cases a nearly axial $S = 3/2$ Fe(II)–NO adduct formed with the E (rhombic) versus D (axial) term $|E/D| \approx 0.010$.

Similarly, anaerobic reconstitution of the proteins with both Fe(II) and a 10-fold excess of the product succinate, followed by addition of NO, led to a single strong resonance signal around $g_{eff} = 3.93$ that contained a slightly higher degree of rhombicity ($|E/D| \approx 0.015$) (Figure 4F). The H169A/D171A protein behaved very differently. After being incubated with Fe(II) under anaerobic conditions, a very strong signal centred at $g \approx 2$ appeared immediately after addition of NO. Only a very weak resonance around $g \approx 4$ could be detected, with small variations in relative intensities from preparation to preparation. These findings confirm that when the histidine-carboxylate Fe-binding region is abrogated, only a much smaller fraction of Fe productively forms stable $S = 3/2$ Fe–NO complexes (Figure 4D). Upon addition of oxygen, the ALKBH4 protein sample that contained 2OG (Figure 4H), and also the sample that was deficient in co-substrate (Figure 4I), displayed formation of strong similar signals with broad shoulders at $g_{eff} = 4.26$, being accompanied by the appearance of weak resonances at $g_{eff} = 9.40$. Those signals originate from transition involving the middle and ground Kramer's doublets respectively and are typically found in high-spin rhombic Fe(III) centres ($|E/D| \approx 0.25$). The same resonances developed in the C15A/C17A mutant upon Fe(II) oxidation. Similarly, a strong signal formed at $g_{eff} = 4.28$ upon oxidation of the Fe(II) H169A/D171A mutant (Figure 4G). However, the presence of broad shoulders like those of the Fe(III) forms of both ALKBH4 and the C15A/C17A mutant were not detected. Such EPR resonance can therefore be interpreted as arising from spurious or non-specifically bound Fe(III) metal ion. Surprisingly, addition of oxygen to the metal-reconstituted ALKBH4 and C15A/C17A proteins in the presence of succinate resulted in protein precipitation. The reason for this is presently unknown.

Motivated by the possibility that the N-terminal cysteine-rich motif might provide an Fe–S cluster, we measured the EPR spectrum of ALKBH4 in the presence of inorganic S and Fe(II).

Table 1 X-band EPR data obtained at $T = 8.0 \pm 0.5$ K for ALKBH4 and mutant proteins (H169A/D171A and C15A/C17A), in their purified forms, after Fe-metal reconstitution in the presence or absence of 2OG/succinate and upon interaction with NO

D, axial ZFS term; *E*, rhombic ZFS term; n.d., not determined; *S*, electronic spin state associated with the individual paramagnetic centre (in parentheses/square brackets).

Protein	Observed EPR *g*-values	$\|E/D\|$	*S*	Notes
ALKBH4 purified[a,b]	4.30 [Fe(III)], 2.10 [Cu(II)]	~1/3	5/2 [Fe(III)], 1/2 [Cu(II)]	Fe(III) and Cu(II) traces
ALKBH4/Fe(II)[a,b]	2.00	n.d.	2 [Fe(II)], 1/2 ($MV^{\bullet+}$)	Recorded under reducing conditions ($Na_2S_2O_4$) in the presence of $MV^{\bullet+}$. Fe(II) was not EPR-visible at X-band; $MV^{\bullet+}$ was EPR active
ALKBH4/Fe(II)/NO[a]	4.08, 3.97, 2.00	0.010	3/2 [Fe(II)–NO complex]	Recorded under reducing conditions ($Na_2S_2O_4$)
ALKBH4/Fe(II)/2OG/NO[a]	4.08, 3.97, 2.00	0.010	3/2 [Fe(II)–NO complex]	Recorded under reducing conditions ($Na_2S_2O_4$)
ALKBH4/Fe(II)/succinate/NO[a]	4.10, 3.93, 2.00	0.015	3/2 [Fe(II)–NO complex]	Recorded under reducing conditions ($Na_2S_2O_4$)
H169A/D171A/Fe(II)/NO	~4.00, 2.02	n.d.	3/2 [Fe(II)–NO complex], 1/2 ($NO^{\bullet}$ radical)	Recorded under reducing conditions ($Na_2S_2O_4$); $NO^{\bullet}$ radical was the major species, Fe(II)–NO complex was a minor species
ALKBH4/Fe(III)/2OG/Na_2S[a]	8.24, 5.56, 4.26, 2.10	0.120	5/2 [Fe(III)], 1/2 [Cu(II)]	Transient species within the Fe(II)→Fe(III) oxidation process. Cu(II) was a minor species
ALKBH4/Fe(III)[a]	9.40, 4.26, 2.10	0.250	5/2 [Fe(III)], 1/2 [Cu(II)]	Cu(II) was a minor species
H169A/D171A/Fe(III)	4.28, 2.10	1/3	5/2 [Fe(III)], 1/2 [Cu(II)]	Non-specifically bound Fe(III). Cu(II) was a minor species
ALKBH4/Fe(III)/2OG[a]	9.40, 4.26, 2.10	0.250	5/2 [Fe(III)], 1/2 [Cu(II)]	Cu(II) was a minor species
ALKBH4/Fe(III)/succinate[a]	n.d.	n.d.	n.d.	Protein precipitation

[a]The same features were observed for the C15A/C17A mutant protein.
[b]The same features were observed for the H169A/D171A mutant protein.

Anaerobic incubation of ALKBH4 with 2OG and Fe(II) in the presence of Na_2S (10-fold excess), followed by addition of O_2 and fast quenching at liquid-N_2 temperature (77 K, –196 °C), resulted in a transient EPR-active species that exhibited resonances at $g_{eff} = 8.24$, 5.56 and 4.26 (Figure 5). Upon thawing, this new species relaxed fast (~20 s) to the high-spin rhombic Fe(III) ion with $|E/D| \approx 0.25$, showing resonances similar to those described in Figure 4(H). Identical behaviour was observed for the C15A/C17A mutant, but not for the mutant H169A/D171A. These effects suggest that the structural changes occuring in the active site within the Fe(II)→Fe(III) oxidation process are modulated further by the presence of Na_2S. It is important to note that similar signals and a similar decay process have been reported in the non-haem Fe(III) centre present in photosystem II, for example, decrease of the $g_{eff} = 8.07$ and $g_{eff} = 5.58$ signals being accompanied by induction (increase) of the signal at the $g_{eff} = 4.26$ signal, as a result of UV-B irradiation (280–320 nm) [37,38]. These types of resonances have previously been analysed by Weisser et al. [39] in terms of ZFS-distributed $S = 5/2$ systems in Fe–catecholato complexes containing moderate rhombic distortion ($|E/D| \approx 0.12$). Furthermore, EPR spectra similar to those reported in Figure 5, although not transient, are observed in Fe(III)–catecholato complexes as model systems of intradiol-cleaving catechol dioxygenases [40], in PAH (phenylalanine hydroxylase) in the presence of catecholamine feedback inhibitors or even when recording PAH in Tris buffer [41,42].

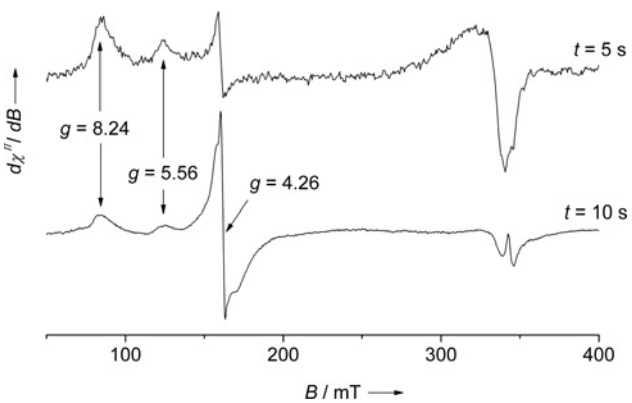

Figure 5 Transient EPR spectra of ALKBH4 recorded within the Fe(II)→Fe(III) oxidation process

X-band EPR spectra of ALKBH4 (120 μM in 50 mM Hepes, pH 7.0) reconstituted with stoichiometric amounts of Fe(II), 2OG (10-fold excess) and Na_2S (10-fold excess), recorded after addition of O_2 followed by quenching after $t = 5$ s (upper trace) or $t = 10$ s (lower trace) of the ice-cooled solutions down to liquid-N_2 temperature ($T = 77$ K). The measurements were performed at $T = 8.0 \pm 0.5$ K; frequency, 9.67 GHz; modulation frequency, 100 KHz; modulation amplitude, 0.7 mT; gain, 55 dB; time constant, 81.92 ms; sweep time, 323 s; microwave power, 0.8 mW; cavity quality factor $Q = 4200$–4400; two scans were accumulated and averaged.

The optical signatures of ALKBH4 and mutant proteins probed by UV–Vis absorption spectroscopy

In parallel with the low-temperature EPR experiments, the optical fingerprints of the various forms of ALKBH4 and mutants [Fe(II)/Fe(III) in the presence of, and without, 2OG] were probed by UV–Vis absorption spectroscopy. The electronic spectrum of the purified ALKBH4 protein did not show absorption features in the visible region (Figure 6A, dashed line). Similarly, the C15A/C17A and H169A/D171A proteins gave featureless spectra. Upon reconstitution with Fe(II), but in the absence of 2OG, both ALKBH4 and the C15A/C17A mutant developed a broad and composite absorption band, extending from 400 nm ($\lambda = 404$ nm, $\varepsilon \approx 570$ $M^{-1} \cdot cm^{-1}$) to 600 nm ($\lambda = 490$ nm, $\varepsilon \approx 260$ $M^{-1} \cdot cm^{-1}$) (Figure 6A, dashed and dotted line). However, the strong absorption band around 320 nm, due to the presence of $Na_2S_2O_4$ (reducing equivalents) in the medium, masked an additional high-energy absorption signature, around 350 nm ($\varepsilon \approx 920$ $M^{-1} \cdot cm^{-1}$), as substantiated in those samples reconstituted with Fe(II) without the supply of reducing agents (Figure 6A, continuous line). When a 10-fold excess of 2OG was added under reducing conditions, a slightly different chromophore ($\lambda = 430$ nm, $\varepsilon \approx 440$ $M^{-1} \cdot cm^{-1}$) developed quickly in both ALKBH4/Fe(II) and the C15A/C17A/Fe(II) protein (Figure 6B, dotted line), with an absorption envelope similar to that observed by Henshaw et al. [43] in *E. coli* AlkB in the presence of Fe(II)/2OG. Upon oxidation, both ALKBH4/Fe(II) and the C15A/C17A/Fe(II) mutant showed the formation of an

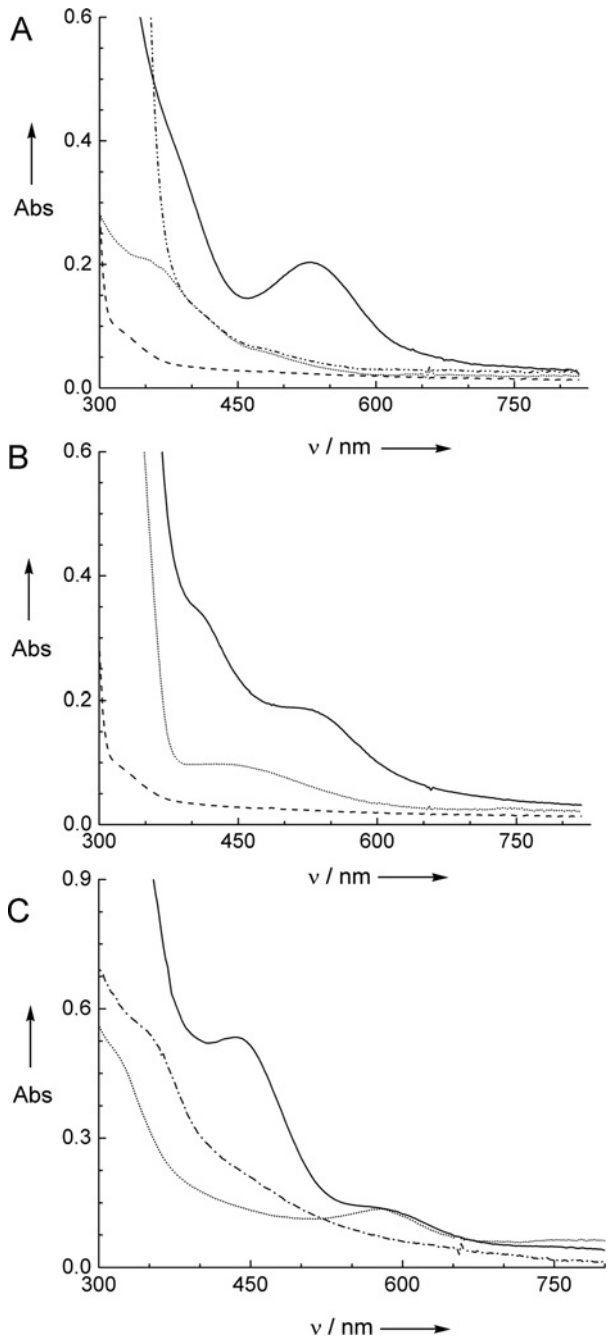

Figure 6 UV–Vis absorption spectroscopy of Fe-reconstituted ALKBH4

(**A**) Purified ALKBH4 (dashed line), ALKBH4/Fe(II) recorded under anaerobic conditions in the absence of $Na_2S_2O_4$ (dotted line), and ALKBH4/Fe(II) recorded under anaerobic conditions in the presence of $Na_2S_2O_4$ (dashed and dotted line) and after oxidation (continuous line). (**B**) ALKBH4/Fe(II)/2OG recorded under anaerobic conditions in the presence of $Na_2S_2O_4$ (dotted line) and after oxidation (continuous line). Note that the spectrum showing the optical feature of purified ALKBH4 (dashed line) from (**A**) is also included here for easier comparison. (**C**) ALKBH4/Fe(II)/2OG recorded in the presence of $Na_2S_2O_4$ after addition of NO gas under anaerobic conditions (continuous line) and after oxidation (dotted line). The corresponding spectrum of the H169A/D171A mutant [incubated with Fe(II) and 2OG] after NO exposure under anaerobic conditions is shown as a dashed line. Protein concentrations were 0.22 mM in 50 mM Hepes, pH 7.0, cooled solutions ($T \leqslant 10\,^{\circ}C$). Abs, absorbance.

absorption band centred at 530 nm ($\varepsilon \approx 920\ M^{-1} \cdot cm^{-1}$), being accompanied by the appearance of a shoulder at higher energy ($\lambda_{max} = 370$ nm, $\varepsilon \approx 2000\ M^{-1} \cdot cm^{-1}$) (Figure 6A, continuous line). Similarly, upon oxidation of Fe(II)- and 2OG-reconstituted ALKBH4 and C15A/C17A protein, an absorption band that was slightly blue-shifted ($\lambda_{max} = 520$ nm, $\varepsilon \approx 860\ M^{-1} \cdot cm^{-1}$) was detected together with a shoulder at $\lambda_{max} = 404$ nm ($\varepsilon \approx 1580\ M^{-1} \cdot cm^{-1}$) (Figure 6B, continuous line). None of the above-reported absorptions were observed in the H169A/D171A mutant, neither in the Fe-reduced nor -oxidized state. Reconstitution of ALKBH4 and the C15A/C17A protein with a 5-fold excess of Fe(II) metal ions prior to oxidation did not result in any further increase of the absorption features in the visible regions. These findings reinforce the hypothesis that (i) ALKBH4 is mononuclear in Fe content, (ii) the cysteine-rich N-terminal site does not provide an additional binding centre for the Fe(II)/Fe(III) metal ion, and furthermore (iii) an intact histidine-carboxylate site is necessary for productive Fe binding, in agreement with the results obtained in the 2OG-decarboxylation-activity assay. Since the optical features of both ALKBH4 and the C15A/C17A protein are clearly modulated by the presence of 2OG, these differences may indeed mirror modifications in the Fe co-ordination environment upon interaction with the substrate, such as the displacement of previously co-ordinated water molecules to the metal Fe. In the present study, the development of rather strong chromophores around 520–530 nm in the Fe(III) ALKBH4 and C15A/C17A protein forms closely resemble the optical spectra observed in synthetic models of non-haem Fe(III)–catecholato/phenolato complexes [40]. Therefore the spectroscopic behaviour displayed especially for the Fe(III) forms of ALKBH4 and the C15A/C17A mutant is different from that previously observed for analogous non-haem Fe proteins, such as AlkB and the Fe(II)/2OG-dependent TauD (taurine dioxygenase). AlkB exhibits an absorption band at $\lambda_{max} = 560$ nm ($\varepsilon = 1258\ M^{-1} \cdot cm^{-1}$) [44] or, as found in other reports [12,43], a much weaker broad band at 450–500 nm, whereas TauD shows an absorption band at $\lambda_{max} = 530$ nm ($\varepsilon = 140\ M^{-1} \cdot cm^{-1}$) [45], when both 2OG and Fe(II) are present under strict anaerobic conditions. In these proteins, exposure to oxygen in the absence of primary substrate causes the development of greenish-brown chromophores. In TauD ($\lambda_{max} = 550$ nm, $\varepsilon = 700\ M^{-1} \cdot cm^{-1}$), the absorption envelope in the oxidized protein arises from a self-hydroxylation reaction of a tyrosine residue (Tyr^{73}) near the non-haem metal site [45]. In AlkB, the formation of a greenish-brown chromophore upon oxidation ($\lambda_{max} = 595$ nm, $\varepsilon = 960\ M^{-1} \cdot cm^{-1}$) indicates a similar self-hydroxylation process that involves Trp^{178} [43]. In order to further study the O_2-binding properties of ALKBH4, we followed the optical changes of the Fe(II) metal core upon interaction with the dioxygen analogue NO, as performed in the EPR experiments reported earlier. Addition of NO to an anaerobic solution of ALKBH4 containing Fe(II), 2OG and $Na_2S_2O_4$ produced a strong yellowish-green chromophore, with a broad absorption band around 580 nm ($\varepsilon \approx 620\ M^{-1} \cdot cm^{-1}$) being accompanied by a more intense peak at 436 nm ($\varepsilon \approx 2430\ M^{-1} \cdot cm^{-1}$) (Figure 6C, continuous line). A similar spectrum was obtained for the C15A/C17A mutant (results not shown). These optical features closely resemble those reported for other non-haem Fe proteins [46] anaerobically treated with NO, such as PAH ($\lambda_{max} = 440$ nm, $\varepsilon \approx 2300\ M^{-1} \cdot cm^{-1}$) in the presence of its co-substrate tetrahydropterin [47], which exhibits, in addition, similar EPR resonance to our NO complex. However, after injection of oxygen, the Fe(II)–NO adduct decayed into a greenish-brown chromophore ($\lambda = 580$ nm, $\varepsilon \approx 620\ M^{-1} \cdot cm^{-1}$, and $\lambda = 770$ nm, $\varepsilon \approx 270\ M^{-1} \cdot cm^{-1}$) (Figure 6C, dotted line), without recovery of the optical features for the Fe(III) form shown previously (Figure 6B, continuous line). This might indicate that the protein becomes more sensitive towards side

reactions upon NO binding and subsequent oxidation, since the recorded envelope in this case is very similar to the one observed in AlkB upon Trp^{178} hydroxylation [43]. Large differences can also be seen between ALKBH4 (and the C15A/C17A mutant) and the H169A/D171A mutant with respect to NO reactivity. After addition of NO to the colourless solution of the H169A/D171A/Fe(II)/2OG protein under anaerobic conditions, a yellowish solution formed without the emergence of any of the Fe–NO characteristic absorption bands, apart from a very broad absorption envelope, extending from 350 nm to 700 nm (Figure 6C, dashed and dotted line). This result supports the previous observation from the low-temperature EPR spectra (Figure 4D) that only a minor amount of Fe–NO adduct can be formed in the case of the H169A/D171A mutant, with the majority of the supplied Fe metal ions non-specifically bound to the protein.

Conclusions

In the present work, we have addressed the characteristics (electronic and magnetic) of the Fe metal core in the human AlkB homologue ALKBH4, and we have shown that an intact His^{169}-Asp^{171}-His^{254} motif is necessary for productive Fe binding and for decarboxylation activity towards 2OG. Furthermore, we have shown that the N-proximal cysteine-rich motif of ALKBH4 is not involved in Fe binding. Although the biological function of ALKBH4 remains elusive, its ability to bind and decarboxylate 2OG after metal reconstitution, together with the optical and spectroscopic fingerprints of its suggested catalytic centre, confirm for the first time that ALKBH4 truly belongs to the class of 2OG-dependent mononuclear non-haem Fe proteins. Additional work is needed to determine the nature of the transient species detected within the reoxidation process in the presence of Na_2S.

AUTHOR CONTRIBUTION

Linn Bjørnstad planned experiments, produced wild-type and mutant proteins, undertook activity measurement, analysed all of the results and wrote the manuscript. Giorgio Zoppellaro planned experiments, performed EPR and light-absorption experiments, analysed all of the results and wrote the manuscript. Ane Tomter performed EPR experiments, analysed results and wrote the manuscript. Pål Falnes designed wild-type protein and mutants, provided experience in AlkB protein, analysed all of the results and wrote the manuscript. Kristoffer Andersson planned physical chemistry experiments, provided experience in non-haem Fe proteins, analysed all of the results and wrote the manuscript.

FUNDING

This work was supported by the PEOPLE Marie Curie Actions Intra-European Fellowship within the 7th European Community Framework Programme [grant number PIEF-GA-2009-235237 (to G.Z.)], the Norwegian Cancer Society [grant number PR-2007-0132 (to L.G.B.)], the Research Council of Norway [FUGE program grant number 159013/S10 (to P.Ø.F.) and grant number 177661/V30 (to K.K.A.)] and the Polish-Norwegian Research Fund [grant number PNRF-143-AI-1/07 (to P.Ø.F.)].

REFERENCES

1 Costas, M., Mehn, M. P., Jensen, M. P. and Que, Jr, L. (2004) Dioxygen activation at mononuclear nonheme iron active sites: enzymes, models, and intermediates. Chem. Rev. **104**, 939–986
2 Schofield, C. J. and Zhang, Z. (1999) Structural and mechanistic studies on 2-oxoglutarate-dependent oxygenases and related enzymes. Curr. Opin. Struct. Biol. **9**, 722–731
3 Neidig, M. L., Brown, C. D., Light, K. M., Fujimori, D. G., Nolan, E. M., Price, J. C., Barr, E. W., Bollinger, Jr, J. M., Krebs, C., Walsh, C. T. and Solomon, E. I. (2007) CD and MCD of CytC3 and taurine dioxygenase: role of the facial triad in α-KG-dependent oxygenases. J. Am. Chem. Soc. **129**, 14224–14231
4 Price, J. C., Barr, E. W., Tirupati, B., Bollinger, Jr, J. M. and Krebs, C. (2003) The first direct characterization of a high-valent iron intermediate in the reaction of an α-ketoglutarate-dependent dioxygenase: a high-spin Fe(IV) complex in taurine/α-ketoglutarate dioxygenase (TauD) from *Escherichia coli*. Biochemistry **42**, 7497–7508
5 Que, Jr, L., and Ho, R. Y. (1996) Dioxygen activation by enzymes with mononuclear non-heme iron active sites. Chem. Rev. **96**, 2607–2624
6 Hegg, E. L. and Que, Jr, L. (1997) The 2-His-1-carboxylate facial triad – an emerging structural motif in mononuclear non-heme iron(II) enzymes. Eur. J. Biochem. **250**, 625–629
7 Neidig, M. L., Kavana, M., Moran, G. R. and Solomon, E. I. (2004) CD and MCD studies of the non-heme ferrous active site in (4-hydroxyphenyl)pyruvate dioxygenase: correlation between oxygen activation in the extradiol and α-KG-dependent dioxygenases. J. Am. Chem. Soc. **126**, 4486–4487
8 Purpero, V. and Moran, G. R. (2007) The diverse and pervasive chemistries of the α-keto acid dependent enzymes. J. Biol. Inorg. Chem. **12**, 587–601
9 Zhou, J., Gunsior, M., Bachmann, B. O., Townsend, C. A. and Solomon, E. I. (1998) Substrate binding to the α-ketoglutarate-dependent non-heme iron enzyme clavaminate synthase 2: coupling mechanism of oxidative decarboxylation and hydroxylation. J. Am. Chem. Soc. **120**, 13539–13540
10 Valegard, K., van Scheltinga, A. C., Lloyd, M. D., Hara, T., Ramaswamy, S., Perrakis, A., Thompson, A., Lee, H. J., Baldwin, J. E., Schofield, C. J. et al. (1998) Structure of a cephalosporin synthase. Nature **394**, 805–809
11 Falnes, P. O., Johansen, R. F. and Seeberg, E. (2002) AlkB-mediated oxidative demethylation reverses DNA damage in *Escherichia coli*. Nature **419**, 178–182
12 Trewick, S. C., Henshaw, T. F., Hausinger, R. P., Lindahl, T. and Sedgwick, B. (2002) Oxidative demethylation by *Escherichia coli* AlkB directly reverts DNA base damage. Nature **419**, 174–178
13 Delaney, J. C., Smeester, L., Wong, C., Frick, L. E., Taghizadeh, K., Wishnok, J. S., Drennan, C. L., Samson, L. D. and Essigmann, J. M. (2005) AlkB reverses etheno DNA lesions caused by lipid oxidation *in vitro* and *in vivo*. Nat. Struct. Mol. Biol. **12**, 855–860
14 Falnes, P. O. (2004) Repair of 3-methylthymine and 1-methylguanine lesions by bacterial and human AlkB proteins. Nucleic Acids Res. **32**, 6260–6267
15 Frick, L. E., Delaney, J. C., Wong, C., Drennan, C. L. and Essigmann, J. M. (2007) Alleviation of 1,N^6-ethanoadenine genotoxicity by the *Escherichia coli* adaptive response protein AlkB. Proc. Natl. Acad. Sci. U.S.A. **104**, 755–760
16 Koivisto, P., Robins, P., Lindahl, T. and Sedgwick, B. (2004) Demethylation of 3-methylthymine in DNA by bacterial and human DNA dioxygenases. J. Biol. Chem. **279**, 40470–40474
17 Mishina, Y., Yang, C. G. and He, C. (2005) Direct repair of the exocyclic DNA adduct 1,N^6-ethenoadenine by the DNA repair AlkB proteins. J. Am. Chem. Soc. **127**, 14594–14595
18 Falnes, P. O., Klungland, A. and Alseth, I. (2007) Repair of methyl lesions in DNA and RNA by oxidative demethylation. Neuroscience **145**, 1222–1232
19 Aravind, L. and Koonin, E. V. (2001) The DNA-repair protein AlkB, EGL-9, and leprecan define new families of 2-oxoglutarate- and iron-dependent dioxygenases. Genome Biol. **2**, RESEARCH0007
20 Han, Z., Niu, T., Chang, J., Lei, X., Zhao, M., Wang, Q., Cheng, W., Wang, J., Feng, Y. and Chai, J. (2010) Crystal structure of the FTO protein reveals basis for its substrate specificity. Nature **464**, 1205–1209
21 Gerken, T., Girard, C. A., Tung, Y. C., Webby, C. J., Saudek, V., Hewitson, K. S., Yeo, G. S., McDonough, M. A., Cunliffe, S., McNeill, L. A. et al. (2007) The obesity-associated *FTO* gene encodes a 2-oxoglutarate-dependent nucleic acid demethylase. Science **318**, 1469–1472
22 Westbye, M. P., Feyzi, E., Aas, P. A., Vagbo, C. B., Talstad, V. A., Kavli, B., Hagen, L., Sundheim, O., Akbari, M., Liabakk, N. B. et al. (2008) Human AlkB homolog 1 is a mitochondrial protein that demethylates 3-methylcytosine in DNA and RNA. J. Biol. Chem. **283**, 25046–25056
23 Duncan, T., Trewick, S. C., Koivisto, P., Bates, P. A., Lindahl, T. and Sedgwick, B. (2002) Reversal of DNA alkylation damage by two human dioxygenases. Proc. Natl. Acad. Sci. U.S.A. **99**, 16660–16665
24 Ringvoll, J., Moen, M. N., Nordstrand, L. M., Meira, L. B., Pang, B., Bekkelund, A., Dedon, P. C., Bjelland, S., Samson, L. D., Falnes, P. O. and Klungland, A. (2008) AlkB homologue 2-mediated repair of ethenoadenine lesions in mammalian DNA. Cancer Res. **68**, 4142–4149
25 Ringvoll, J., Nordstrand, L. M., Vagbo, C. B., Talstad, V., Reite, K., Aas, P. A., Lauritzen, K. H., Liabakk, N. B., Bjork, A., Doughty, R. W. et al. (2006) Repair deficient mice reveal mABH2 as the primary oxidative demethylase for repairing 1meA and 3meC lesions in DNA. EMBO J. **25**, 2189–2198

26 Fu, D., Brophy, J. A., Chan, C. T., Atmore, K. A., Begley, U., Paules, R. S., Dedon, P. C., Begley, T. J. and Samson, L. D. (2010) Human AlkB homolog ABH8 is a tRNA methyltransferase required for wobble uridine modification and DNA damage survival. Mol. Cell. Biol. **30**, 2449–2459

27 Fu, Y., Dai, Q., Zhang, W., Ren, J., Pan, T. and He, C. (2010) The AlkB domain of mammalian ABH8 catalyzes hydroxylation of 5-methoxycarbonylmethyluridine at the wobble position of tRNA. Angew. Chem. Int. Ed. **49**, 1–5

28 Songe-Moller, L., van den Born, E., Leihne, V., Vagbo, C. B., Kristoffersen, T., Krokan, H. E., Kirpekar, F., Falnes, P. O. and Klungland, A. (2010) Mammalian ALKBH8 possesses tRNA methyltransferase activity required for the biogenesis of multiple wobble uridine modifications implicated in translational decoding. Mol. Cell. Biol. **30**, 1814–1827

29 Pan, Z., Sikandar, S., Witherspoon, M., Dizon, D., Nguyen, T., Benirschke, K., Wiley, C., Vrana, P. and Lipkin, S. M. (2008) Impaired placental trophoblast lineage differentiation in Alkbh1$^{-/-}$ mice. Dev. Dyn. **237**, 316–327

29a Tidwell, T. T. (2001) William Schlenk: the man behind the flask. Angew. Chem. Int. Ed. **40**, 331–337

30 Solomon, E. I. and Zhang, Y. (1992) The electronic structures of active sites in non-heme iron enzymes. Acc. Chem. Res. **25**, 343–352

31 McCleverty, J. A. (2004) Chemistry of nitric oxide relevant to biology. Chem. Rev. **104**, 403–418

32 Chen, V. J., Orville, A. M., Harpel, M. R., Frolik, C. A., Surerus, K. K., Munck, E. and Lipscomb, J. D. (1989) Spectroscopic studies of isopenicillin N synthase. A mononuclear nonheme Fe^{2+} oxidase with metal coordination sites for small molecules and substrate. J. Biol. Chem. **264**, 21677–21681

33 Arciero, D. M. and Lipscomb, J. D. (1986) Binding of ^{17}O-labeled substrate and inhibitors to protocatechuate 4,5-dioxygenase-nitrosyl complex. Evidence for direct substrate binding to the active site Fe^{2+} of extradiol dioxygenases. J. Biol. Chem. **261**, 2170–2178

34 Arciero, D. M., Orville, A. M. and Lipscomb, J. D. (1985) [^{17}O]Water and nitric oxide binding by protocatechuate 4,5-dioxygenase and catechol 2,3-dioxygenase. Evidence for binding of exogenous ligands to the active site Fe^{2+} of extradiol dioxygenases. J. Biol. Chem. **260**, 14035–14044

35 Chiou, Y.-M. and Que, Jr, L. (1995) Model studies of α-keto acid-dependent nonheme iron enzymes: nitric oxide adducts of Fe^{II}(L)(O2CCOPh)(ClO4) complexes. Inorg. Chem. **34**, 3270–3278

36 Arciero, D. M., Lipscomb, J. D., Huynh, B. H., Kent, T. A. and Munck, E. (1983) EPR and Mossbauer studies of protocatechuate 4,5-dioxygenase. Characterization of a new Fe^{2+} environment. J. Biol. Chem. **258**, 14981–14991

37 McEvoy, J. P. and Brudvig, G. W. (2008) Redox reactions of the non-heme iron in photosystem II: an EPR spectroscopic study. Biochemistry **47**, 13394–13403

38 Vass, I., Sass, L., Spetea, C., Bakou, A., Ghanotakis, D. F. and Petrouleas, V. (1996) UV-B-induced inhibition of photosystem II electron transport studied by EPR and chlorophyll fluorescence. Impairment of donor and acceptor side components. Biochemistry **35**, 8964–8973

39 Weisser, J. T., Nilges, M. J., Sever, M. J. and Wilker, J. J. (2006) EPR investigation and spectral simulations of iron-catecholate complexes and iron-peptide models of marine adhesive cross-links. Inorg. Chem. **45**, 7736–7747

40 Bruijnincx, P. C., Lutz, M., Spek, A. L., Hagen, W. R., van Koten, G. and Gebbink, R. J. (2007) Iron(III)-catecholato complexes as structural and functional models of the intradiol-cleaving catechol dioxygenases. Inorg. Chem. **46**, 8391–8402

41 Hagedoorn, P.-L., Schmidt, P. P., Andersson, K. K., Hagen, W. R., Flatmark, T. and Martínez, A. (2001) The effect of substrate, dihydrobiopterin, and dopamine on the EPR spectroscopic properties and the midpoint potential of the catalytic iron in recombinant human phenylalanine hydroxylase. J. Biol. Chem. **276**, 22850–22856

42 Martinez, A., Andersson, K. K., Haavik, J. and Flatmark, T. (1991) Recombinant human tyrosine hydroxylase isozymes. Reconstruction with iron and inhibitory effect of other metal ions. Eur. J. Biochem. **198**, 675–682

43 Henshaw, T. F., Feig, M. and Hausinger, R. P. (2004) Aberrant activity of the DNA repair enzyme AlkB. J. Inorg. Biochem. **98**, 856–861

44 Mishina, Y., Chen, L. X. and He, C. (2004) Preparation and characterization of the native iron(II)-containing DNA repair AlkB protein directly from *Escherichia coli*. J. Am. Chem. Soc. **126**, 16930–13936

45 Ryle, M. J., Liu, A., Muthukumaran, R. B., Ho, R. Y., Koehntop, K. D., McCracken, J., Que, Jr, L. and Hausinger, R. P. (2003) O_2- and α-ketoglutarate-dependent tyrosyl radical formation in TauD, an α-keto acid-dependent non-heme iron dioxygenase. Biochemistry **42**, 1854–1862

46 Orville, A. M. and Lipscomb, J. D. (1993) Simultaneous binding of nitric oxide and isotopically labeled substrates or inhibitors by reduced protocatechuate 3,4-dioxygenase. J. Biol. Chem. **268**, 8596–8607

47 Han, A. Y., Lee, A. Q. and Abu-Omar, M. M. (2006) EPR and UV–vis studies of the nitric oxide adducts of bacterial phenylalanine hydroxylase: effects of cofactor and substrate on the iron environment. Inorg. Chem. **45**, 4277–4283

48 Katoh, K., Kuma, K., Toh, H. and Miyata, T. (2005) MAFFT version 5: improvement in accuracy of multiple sequence alignment. Nucleic. Acids Res. **33**, 511–518

49 Waterhouse, A. M., Procter, J. B., Martin, D. M., Clamp, M. and Barton, G. J. (2009) Jalview Version 2 – a multiple sequence alignment editor and analysis workbench. Bioinformatics **25**, 1189–1191

50 Yu, B., Edstrom, W. C., Benach, J., Hamuro, Y., Weber, P. C., Gibney, B. R. and Hunt, J. F. (2006) Crystal structures of catalytic complexes of the oxidative DNA/RNA repair enzyme AlkB. Nature **439**, 879–884

Received 11 October 2010/14 December 2010; accepted 20 December 2010
Published as BJ Immediate Publication 20 December 2010, doi:10.1042/BJ20101667